

## Structure of isovector spin excitations in nuclei

N. Auerbach

*Los Alamos National Laboratory, Los Alamos, New Mexico 87545  
and Department of Physics and Astronomy, Tel-Aviv University, Tel-Aviv, Israel*

Amir Klein

*Department of Physics and Astronomy, Tel-Aviv University, Tel-Aviv, Israel  
(Received 17 October 1983)*

The charge-exchange Hartree-Fock random-phase approximation theory is employed in the calculation of isovector spin excitations in nuclei with  $N > Z$ . Distributions of strength for all three  $\Delta\tau_z = 0, \pm 1$  components of  $S=1$ ,  $L=0, 1, 2$ ,  $J=0^-, 1^-, 2^-, 1^+, 2^+$ , and  $3^+$  excitations are calculated. The results for isotopes of Ni and Zr are also presented.

### I. INTRODUCTION

During the 1970's, new types of giant electric resonances were discovered in addition to the giant dipole which had been known for a long time. These resonances have added new and very interesting information concerning nuclear collective motion, in which only spatial degrees of freedom of nucleons are involved. In the 1980's giant resonances have been observed in which spin degrees of freedom of the nucleons determine the collective properties of these excitations. The long-predicted Gamow-Teller (GT) resonance was observed<sup>1</sup> in (p,n) reactions and recently also the  $M1$  state<sup>2</sup> was seen in (p,p') and (e,e') experiments.<sup>3</sup> Giant resonances in which both spatial and spin degrees of freedom participate, such as the spin dipole ( $L=1$ ,  $S=1$ ) or spin quadrupole ( $L=2$ ,  $S=1$ ), have been studied in (p,n) reactions.<sup>4</sup>

The (p,n) reaction in the energy range of several hundred MeV is particularly well suited for the study of spin excitations in nuclei because of the relatively strong  $T=1$  and  $S=1$  component in the nucleon-nucleon force in this energy range. For energies in the range 100–300 MeV, the (p,n) reaction excites  $\Delta S=1$  excitations preferentially as opposed to the  $\Delta S=0$  excitations which are rather weak.<sup>5</sup> The Gamow-Teller resonance was clearly observed in many nuclei throughout the Periodic Table in the (p,n) reactions.<sup>1,4</sup> The most exciting feature of these experiments was the fact that a large portion of the strength related to the  $\sigma\tau$  operator is missing. This observation confirmed the earlier ones that much of the strength is missing from the GT  $\beta^-$  transitions in light nuclei. In the recent (p,p') (Refs. 2, 6, and 7) and in some (e,e') experiments<sup>3</sup>  $M1$  strength was found in medium-mass nuclei. The isovector  $M1$  strength exhausts only about 30–50% of the shell-model strength. In heavy nuclei (as for example in <sup>208</sup>Pb) only a very small fraction of the isovector  $M1$  strength is detected. These experiments together with the charge exchange results point to the fact that a large portion of the shell-model  $\sigma\tau$  strength is missing from the low-energy region.

To resolve this problem an interesting suggestion was put forward, namely, that the quenching of the  $\sigma\tau$

strength is due to the excitation of internal degrees of freedom of a nucleon.<sup>8</sup> This quenching is probably one of the most natural and straightforward manifestations of the coupling of non-nucleonic degrees of freedom to the nucleonic ones in a nucleus. Because of the Pauli principle very few nucleons can flip their spin without a change in their spatial degrees of freedom. On the other hand, each of the nucleons in a nucleus can be excited into a  $\Delta_{33}$  which occupies the same or nearly the same state as the initial nucleon. In the language of quarks each nucleon in the nucleus can flip the spin of one of its quarks, thus aligning the three quark spins. This spin flip must be accompanied by an isospin flip too, so that the state is symmetric in spin and isospin of the quarks. Although the admixture of a  $\Delta$ -particle–nucleon-hole state  $|\Delta N^{-1}\rangle$  into the nuclear  $M1$  or  $GT$  is small (it costs 300 MeV to excite a nucleon into a delta), because of the coherence of the  $|\Delta N^{-1}\rangle$  and therefore the large transition strength to such a state, the effect on the  $M1$  or  $GT$  strength is large.<sup>8</sup> This explanation of the missing isovector spin-flip strength in the low-lying states of nuclei is quite convincing; however, other possibilities cannot be excluded, and additional contributions should be taken into account.<sup>9–13</sup>

In some nuclei the random phase approximation (RPA) correlations might affect the GT strength and certainly the  $M1$  transitions. In a previous work<sup>11</sup> this aspect of theory was studied for the GT and  $M1$  resonances in several nuclei. The excitations corresponding to the  $\sigma\tau_-$ ,  $\sigma\tau_0$ , and  $\sigma\tau_+$  operators were calculated in the same theoretical framework. In the present work we extend these calculations to other isovector-spin excitations involving angular momentum transfer as well. All three components for each kind of isovector transition operator are calculated simultaneously using the theory of charge-exchange RPA.<sup>14</sup> The excitations considered in this work are the isovector  $S=1$ ,  $L=1$ ,  $J=0^-, 1^-, 2^-$  and isovector  $S=1$ ,  $L=2$ ,  $J=1^+, 2^+, 3^+$ . The isovector spin monopole state, i.e., a state which relates to the operator  $r^2\sigma\tau_\mu$ , is also calculated. For completeness the results for the  $L=0$ ,  $S=1$  excitations corresponding to the operator  $\sigma\tau_\mu$  (i.e., the  $M1$ ,  $GT$ , and  $\beta^+$  states) which were calculated in Ref. 11 are presented here and some new results

added. In the present work, we consider only nucleon degrees of freedom and do not treat the coupling to the  $\Delta$ . However, the complete nucleon 1p-1h space is utilized. This includes the continuum particle-hole configurations<sup>15</sup> and therefore we are able to compute the nucleon escape widths of the resulting excitations.

The calculations performed in the framework of the charge-exchange RPA use the proton-particle neutron-hole states to describe the  $\Delta\tau_z = -1$  components of the isovector excitations. The proton particle-proton hole and neutron particle-neutron hole configurations form the  $\Delta\tau_z = 0$  excitations and the  $\Delta\tau_z = 1$  excitations are constructed from the neutron particle-proton hole configurations. The basis of our calculations is made up of Hartree-Fock (HF) single particle (hole) states calculated with Skyrme-type forces.<sup>16,17</sup>

Previous extensive studies of spin-flip excitations included the work in Ref. 18 where the  $\Delta\tau_z = -1$  excitations for  $L = 0$  spin-flip excitations were calculated in the Tamm-Dancoff approximation (TDA) and the  $L = 1$  in the RPA. A simple  $\delta$  force was used for the p-h interaction and both HF and Woods-Saxon single particle states were employed. The  $\Delta\tau_z = -1$  and  $\Delta\tau_z = 0$  were not treated in the above work. In some other papers<sup>10,19</sup> the  $\Delta\tau_z = -1$  excitations have been calculated in a limited 1p-1h basis. Gaarde *et al.*<sup>4</sup> have calculated in addition to the  $L = 0$  and 1 strength also the  $L = 2$  strength, but again only for  $\Delta\tau_z = 1$ , and they did not include continuum states. Full shell-model calculations in a limited space of GT and  $M1$  states have been recently carried out.<sup>20</sup>

The work which comes closest to ours is that of Izumoto in which  $\Delta\tau_z = -1$ ,  $L = 0, 1$ , and 2 excitations are computed in the RPA framework with the 1p-1h continuum states included in the calculation.<sup>21</sup> But again as in previous work there is no attempt to treat all three  $\Delta\tau_z = \pm 1, 0$  components of the isovector spin excitations in the same theoretical framework. The main aim of this work is to provide such unified treatment of isovector spin excitations.

## II. THE FORMALISM

The fundamental quantity of the method used here is the particle-hole Green's function,  $G(E)$ , where  $E$  is the excitation energy.<sup>22</sup> The linear response of the nucleus to a one-body probe  $Q$  can be calculated in coordinate space as

$$S_Q(E) = \frac{1}{\pi} \text{Im} \left[ \int Q^+(\vec{r}') G(\vec{r}, \vec{r}', E) Q(\vec{r}) d\vec{r}' d\vec{r} \right]. \quad (2.1)$$

The transition density  $\rho_n(\vec{r})$  for the excited state  $|n\rangle$  at energy  $E_n$  is unambiguously determined as follows:<sup>23</sup>

$$\rho_n(\vec{r}) = \frac{\frac{1}{\pi} \text{Im} \left[ \int Q^+(\vec{r}') G(\vec{r}, \vec{r}', E_n) \hat{\rho}(\vec{r}) d\vec{r}' d\vec{r} \right]}{\sqrt{S_Q(E_n)}}, \quad (2.2)$$

where  $\hat{\rho}(\vec{r})$  is the one-body density operator.<sup>24</sup>

Our framework consists of a shell-model (HF) Hamiltonian and a residual interaction. The Green's function is obtained by solving the ladder approximation equation

$$G(E) = G^{(0)}(E) - G^{(0)}(E) V_{\text{ph}} G(E). \quad (2.3)$$

$V_{\text{ph}}$  is the particle-hole (residual) interaction which we take to be of static nature, and  $G^{(0)}(E)$  is the free Green's function constructed using HF wave functions and energies. This framework was used in the past<sup>25,26</sup> for systematic studies of electric isoscalar and isovector resonances. It was recently<sup>14</sup> extended to include the charge-exchange ( $\Delta\tau_z = +1$  and  $\Delta\tau_z = -1$ ) components of giant isovector states.

In this work we use the Skyrme III (SIII) effective two-body nucleon-nucleon force<sup>17</sup> in order to generate the HF Hamiltonian. The 1p-1h space we use to construct the free Green's function is complete,<sup>15</sup> and consequently, as already remarked, the excited states lying in the continuum will have particle escape widths. The spreading widths due to 2p-2h or higher order configurations are not treated in our calculations.

The residual p-h interaction may, in principle, be calculated in a *self-consistent manner* by employing Landau's prescription:<sup>22</sup>

$$V_{\text{ph}} \rightarrow \frac{\delta^2 E_{\text{HF}}}{\delta\rho\delta\rho}, \quad (2.4)$$

where  $E_{\text{HF}}$  is the HF energy and  $\delta\rho$  designates a variation in the one-body density function. However, it is well known in the literature that the Skyrme forces SI to SVI (Refs. 16 and 17) (including the SIII force used here in the construction of the HF potential) have some shortcomings in relation to spin-flip excitations.<sup>27-29</sup> The authors of Ref. 29 have tried to determine a few new sets of parameters for the Skyrme interactions. Being interested mainly in the general features of the strength distributions for the three isospin components of magnetic isovector states, we adopted here a simpler approach. The residual interaction was taken to be of zero range and of the form:

$$V_{\text{ph}}(1,2) = t [(1 - P_\sigma P_\tau) + x (P_\sigma - P_\tau)] \delta(\vec{r}_1 - \vec{r}_2), \quad (2.5)$$

where  $P_\sigma, P_\tau$  are the spin and isospin exchange operators and  $t, x$  are two constants to be determined. In expression (2.5) the density-dependent and the velocity-dependent terms and also the spin-orbit term, that appear in a Skyrme force, have been dropped. The value of  $t$  was chosen so as to reasonably reproduce the two GT peaks of  $^{90}\text{Zr}$ ,<sup>30</sup>  $t = -934 \text{ MeV fm}^3$ .

In view of very recent theoretical fits<sup>31</sup> of a measured<sup>32</sup> low energy  $M1$  state in  $^{208}\text{Pb}$ , which indicate that the ratio between the coefficients of the isoscalar spin-flip and the isovector spin-flip terms in the residual interaction is very small, we chose  $x = 0.5$ . The isoscalar spin-flip term of the residual interaction, Eq. (2.5), is zero for this value of  $x$ .

We should mention that the isovector spin-flip term in our  $V_{\text{ph}}$ , which is

$$233.5 \vec{\sigma}_1 \cdot \vec{\sigma}_2 \vec{\tau}_1 \cdot \vec{\tau}_2 \delta(\vec{r}_1 - \vec{r}_2),$$

is close to that used by Bertsch *et al.*<sup>18</sup> Also, our value of  $t$  corresponds to a Landau parameter  $g'_0 = 0.56$  in units of  $\hbar^2 \pi^2 / m^* k_F$ , where  $m^*$  is the effective mass and  $k_F$  is the Fermi momentum in nuclear matter. If the one pion ex-

change potential<sup>33</sup> and the  $\rho$ -exchange potential contributions to the zero-range part of the p-h interaction are included, then the value of  $t$  we used is equivalent to  $g'_0=0.95$ , which is close to values employed by other authors.<sup>21,33,34</sup>

The distributions of strength are calculated for operators possessing the following general form:

$$Q_{L,J,\mu} = i^{L+1-J} \sum_{i=1}^A f(r_i) [Y_L(\hat{r}_i) \times \vec{\sigma}(i)]_{J,0} \tau_\mu(i), \quad (\mu=0, \pm 1) \quad (2.6)$$

where

$$\tau_\mu = \begin{cases} \mp \frac{1}{\sqrt{2}} (\tau_x \pm i\tau_y), & \mu = \pm 1 \\ \tau_z, & \mu = 0 \end{cases} \quad (2.7)$$

and  $\tau_x, \tau_y, \tau_z$  are the Pauli isospin matrices. The strength distribution can be characterized in terms of its moments,

$$m_{L,J,\mu}(k) = \sum_{n_\mu} E_{n_\mu}^k |\langle n_\mu | Q_{L,J,\mu} | 0 \rangle|^2, \quad (\mu=0, \pm 1; k=0, 1, 2, \dots) \quad (2.8)$$

where  $E_{n_\mu}$  is the energy of the state  $|n_\mu\rangle$  excited by the operator  $Q_{L,J,\mu}$  acting on the ground state  $|0\rangle$ . We will also refer to the average excitation energy

$$E_{L,J,\mu} = \frac{m_{L,J,\mu}(1)}{m_{L,J,\mu}(0)}, \quad (\mu=0, \pm 1). \quad (2.9)$$

All energies will be given with respect to the parent ground state.

In the framework of the continuum RPA, the zeroth order moments of the strength distributions corresponding to the charge-exchange modes can be shown to satisfy the following nonenergy weighted sum rule (NEWSR):

$$m_{L,J,-1}(0) - m_{L,J,+1}(0) = \frac{1}{2\pi} [N \langle f^2(r) \rangle_n - Z \langle f^2(r) \rangle_p], \quad (2.10)$$

where  $\langle F(r) \rangle_n$  stands for  $\int d^2\vec{r} F(r) \rho_n(r)$ ,  $\langle F(r) \rangle_p$  stands for  $\int d^2\vec{r} F(r) \rho_p(r)$ , and  $\rho_n, \rho_p$  are the neutron and proton densities, respectively, in the ground state. In particular, taking  $f(r) = r^l$ , we get

$$\text{rhs of Eq. (2.10)} = \frac{1}{2\pi} [N \langle r^{2l} \rangle_n - \langle r^{2l} \rangle_p]. \quad (2.11)$$

The relationship Eq. (2.10) is independent of the specific form of the residual interaction and remains valid also when its lhs is evaluated by using the continuum TDA. We employed the NEWSR in Eqs. (2.10) and (2.11) as a check of the numerical accuracy achieved in our calculations.

### III. RESULTS

We performed complete calculations for the nuclei  $^{60}\text{Ni}$ ,  $^{90}\text{Zr}$ , and  $^{208}\text{Pb}$ . We obtained the Green's function in

coordinate space<sup>25,26</sup> using a radial mesh of 26 points with  $\Delta r = 0.45$  fm for  $^{60}\text{Ni}$  and 0.60 fm for the other two nuclei.

#### A. Results for $L=0$ states: The GT and $M1$ resonances

The probing operator in this case is

$$Q_{0,1^+, \mu} = \sum_{i=1}^A [Y_{00}(\hat{r}_i) \times \vec{\sigma}(i)]_{1,0} \tau_\mu(i) \quad (\mu=0, \pm 1). \quad (3.1)$$

Some of the results of such calculations were reported in Ref. 11. (Note that we use here a probing operator that is  $1/\sqrt{4\pi}$  times the one used in Ref. 3.) Satisfactory agreement with experiment was found concerning excitation energies. Motivated by the recent investigations of the mass dependence of the  $M1$  and GT strength,<sup>6,7,37</sup> we also calculated several isotopes of Ni and Zr. In the Ni isotopes, the two isospin components of  $M1$ , the lower energy  $T'=T$  (the isospin of the parent state) component, and the higher energy  $T'=T+1$  one were identified.<sup>7</sup> Although our calculations are not carried out in a good isospin framework, we can approximately decompose the theoretical  $M1$  strength into isospin components using the  $\sigma\tau_{+1}$  strength.<sup>11,14</sup> The resulting excitation energies, together with the ratio of the reduced strength,  $S_{T+1}/S_T$ , are given in Table I. The latter quantity should give an indication about the expected ratio of the cross sections for exciting the corresponding  $1^+$  levels. The strength of the  $\mu=+1$  mode,  $S_{T+1}$ , is almost entirely due to the  $\pi 1f_{7/2} \rightarrow \nu 1f_{5/2}$  transition. As  $A$  increases, this transition becomes gradually blocked; at the same time,  $S_T$  decreases to a lesser extent, because it is only indirectly affected by the  $1f_{5/2}$  neutrons.

Recently, (p,n) experiments<sup>36,37</sup> on  $^{58}\text{Ni}$  and on even Ni isotopes from  $^{58}\text{Ni}$  through  $^{64}\text{Ni}$  were performed in which Gamow-Teller strength was observed. In Ref. 37 isospin assignments of the  $T+1$ ,  $T$ , and  $T-1$  components have been made. The energy positions compare reasonably well with the calculated ones although the splitting between the  $T+1$  and  $T$  component  $\Delta E_+$  is theoretically somewhat smaller than that measured experimentally. The symmetry energy coefficient defined as  $V_1 = \Delta E_+ A / (T+1)$  is theoretically around 70 MeV, while from the

TABLE I. Excitation energies and the ratio of  $S_{T+1}/S_T$  (see text) for Ni isotopes.

Nucleus	$E_T$ (MeV)	$E_{T+1}$ (MeV)	$S_{T+1}/S_T$
$^{60}\text{Ni}$	9.4 <sup>a</sup>	12.3 <sup>a</sup>	0.70
	$8.9 \pm 0.1$ <sup>b</sup>	$11.7$ <sup>b</sup>	
$^{62}\text{Ni}$	9.0 <sup>a</sup>	12.9 <sup>a</sup>	0.49
	$8.8 \pm 0.1$ <sup>b</sup>	$14.0$ <sup>b</sup>	
$^{64}\text{Ni}$	8.5	13.2	0.26
	$8.9 \pm 0.1$ <sup>b</sup>	$15.6$ <sup>b</sup>	

<sup>a</sup>Theory

<sup>b</sup>Experiment (Ref. 7).

analysis of the experimental (p,n) data<sup>37</sup> it is about 85 MeV.

The theoretical decomposition into  $T+1$ ,  $T$ , and  $T-1$  components in the Ni isotopes is somewhat ambiguous because of the fragmentation in GT strength resulting from the fact that one has two well separated distributions of strength resulting from the splitting between, on the one hand, the  $f_{7/2}^2$  orbit and, on the other, the  $p_{3/2}^3$  and  $f_{5/2}^5$  orbits. The ratio of strength  $S_{T-1}/S_{T+1}$  is calculated to be about 3 in  $^{60}\text{Ni}$ , 5.3 in  $^{62}\text{Ni}$ , and reaches the value of 12.5 in  $^{64}\text{Ni}$ .

As already discussed in our previous work,<sup>11</sup> in the case of the Ni isotopes the RPA correlations affect not only the  $M1$  strength but also the  $\text{GT}(\beta^-)$  strength and of course the  $\beta^+$  transitions. It is the existence of the  $\beta^+$  transitions (which represent the "backward going" graphs for  $\beta^-$ ) that makes the RPA correlations important in the GT strength.<sup>4,11</sup> The reduction of strength due to RPA correlations is for the  $M1$  33% in  $^{60}\text{Ni}$ , 31% in  $^{62}\text{Ni}$ , and 29% in  $^{64}\text{Ni}$ . As for the GT strength, it is diminished as one goes from  $^{60}\text{Ni}$  to  $^{64}\text{Ni}$ , because of the increase of the  $f_{7/2}^2$  to  $f_{5/2}^5$  transition in the  $\beta^+$  branch. In fact, the transition strength in the RPA for  $\beta^+$  is about 15 in  $^{60}\text{Ni}$ , 9 in  $^{62}\text{Ni}$ , and only 4 in  $^{64}\text{Ni}$ . The experimental results<sup>37</sup> indicate that the quenching of strength in the GT transitions in all Ni isotopes is close to a factor of 3 and certainly cannot be accounted for by the RPA correlations alone.

In the Zr isotopes, the  $M1$  is split into two states for  $A > 90$  (due to the additional  $\nu d_{5/2}^5 \rightarrow \nu d_{3/2}^3$  transition) and the GT resonance is split into four peaks ( $\nu 1d_{5/2}^5 \rightarrow \pi 1d_{5/2}^5$  and  $\nu 1d_{5/2}^5 \rightarrow \pi 1d_{3/2}^3$  in addition to the  $\nu 1g_{7/2}^9 \rightarrow \pi 1g_{7/2}^9$  and  $\nu 1g_{7/2}^9 \rightarrow \pi 1g_{5/2}^7$  configurations). The highest energy peaks carry most of the strength, and we list them in Table II together with experimental results.<sup>6</sup> The agreement with measurements is good for the  $M1$  states; however, the calculated GT peaks are higher than experiment by about 2 MeV.

In Figs. 1 and 2, we show the transition densities for the GT states in  $^{90}\text{Zr}$  and  $^{208}\text{Pb}$ . For  $^{90}\text{Zr}$ , the transition densities (properly normalized to the corresponding strengths) for the two GT peaks are given, and for  $^{208}\text{Pb}$ ,

TABLE II. Excitation energies of the  $M1$  and GT states in Zr isotopes.

Nucleus	$M1$ state (MeV)	GT state (MeV)
$^{90}\text{Zr}$	9.2 <sup>a</sup>	17.4 <sup>a</sup>
	8.9±0.2 <sup>b</sup>	15.6 <sup>b</sup>
$^{92}\text{Zr}$	9.1 <sup>a</sup>	16.7 <sup>a</sup>
	8.8±0.1 <sup>b</sup>	14.9 <sup>b</sup>
$^{94}\text{Zr}$	9.05 <sup>a</sup>	16.1 <sup>a</sup>
	8.7±0.1 <sup>b</sup>	13.8 <sup>b</sup>
$^{96}\text{Zr}$	9.0 <sup>a</sup>	15.4
	8.6±0.1 <sup>b</sup>	

<sup>a</sup>Theory

<sup>b</sup>Experiment (Ref. 6).

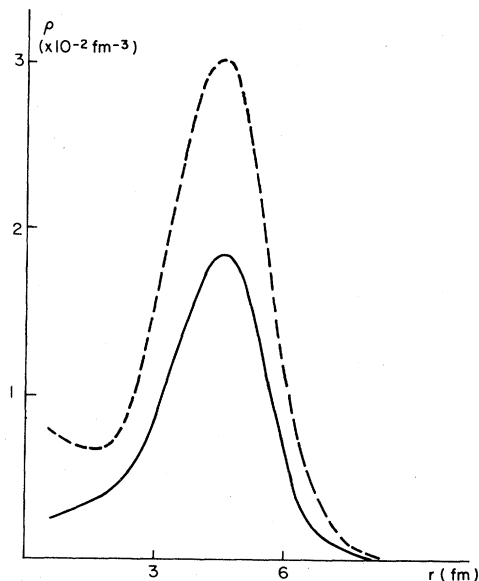


FIG. 1. The transition densities for the two GT peaks in  $^{90}\text{Zr}$ . The continuous line represents the lower energy peak and the dashed line represents the higher energy peak.

the density shown corresponds to the 20.9 MeV peak and it is normalized to the entire strength. We note that the expected resemblance between the GT transition densities and the excess neutron densities is spoiled mainly by the spin-orbit interaction.

#### B. Results for $L=0$ states: The high energy states

Calculations of high-lying  $M1$  resonances were reported in the past.<sup>38</sup> The authors presented estimates of the energies for these states, and their contribution to  $(e,e')$  cross sections at backward angles. Also, very recently,<sup>29</sup> it was pointed out that  $L=0$  strength in the continuum might constitute a significant fraction of the background in the  $^{90}\text{Zr}(p,n)$  reaction.

Because of the absence of radial dependence, the operator  $Q_{0,1+,\mu}$  defined in Eq. (3.1) cannot excite high energy  $L=0$  states. To study them, we define, in analogy with the electric monopole case, the following probe:

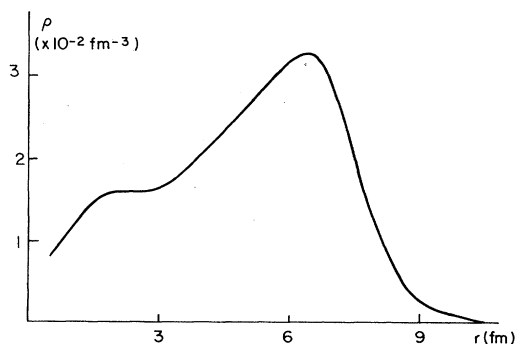


FIG. 2. The transition density for the main peak of the GT distribution in  $^{208}\text{Pb}$ .

$$\bar{Q}_{0,1^+, \mu} = \sum_{i=1}^A r_i^2 [Y_{00}(\hat{r}_i) \times \vec{\sigma}(i)]_{1,0} \tau_{\mu}(i) \quad (\mu=0, \pm 1) \quad (3.2)$$

The functional dependence on  $r$  of  $\bar{Q}_{0,1^+, \mu}$  comes from the long wavelength expansion of  $j_0(qr)$ , where  $q$  is the momentum transfer,

$$j_0(qr) \approx 1 - \frac{q^2 r^2}{6} + \dots \quad (3.3)$$

The probe of Eq. (3.2) excites states of  $1^+$ ,  $L=0$  character, which are built of  $1p-1h$  configurations corresponding to  $2\hbar\omega$  transitions. We will refer to the high-lying  $1^+$ ,  $L=0$  resonances as the *spin isovector monopole* (SIM) resonances.

Let us now discuss the results. The distributions of strength of the operators  $\bar{Q}_{0,1^+, \mu}$  for  $\mu=-1$  and 0 (and for  $^{60}\text{Ni}$ , also  $\mu=+1$ ) exhibit two main concentrations of strength, which are well separated. At the lower energy end, there are the  $GT(\mu=-1)$  and  $M1(\mu=0)$  states. For  $^{60}\text{Ni}$ , there is also the sharp low energy  $0\hbar\omega$  state excited by the  $\mu=+1$  component of  $\bar{Q}_{0,1^+, \mu}$  while for the other nuclei,  $0\hbar\omega$  transitions of this kind are completely blocked by the excess neutrons. These low-energy states carry a large fraction of *total* transition strength of the operator  $\bar{Q}_{0,1^+, \mu}$ : the  $GT$  in  $^{60}\text{Ni}$  and  $^{90}\text{Zr}$  contains about 75% of the total strength, and in  $^{208}\text{Pb}$ , the fraction is 90%. The  $M1$  represents about 60% of the *total strength* of  $\bar{Q}_{0,1^+, 0}$  in the three nuclei. As for the  $\mu=+1$  mode in  $^{60}\text{Ni}$ , the low-energy state carries about 60% of the *total strength*.

The high-energy concentration of strength represents the SIM resonance whose distribution strikingly resembles that of the electric isovector monopole:<sup>14</sup> at its lower energy it is quite fragmented and at the higher energy end there is a strong and wide peak, which contains about 70% of the SIM strength. In Fig. 3 are shown the distributions of strength of the probes  $\bar{Q}_{0,1^+, \mu}$  for the three modes in  $^{90}\text{Zr}$ . We observe that because of the larger escape widths the  $\mu=1$  mode has a smoother shape than the other two modes, with  $\mu=+1, 0$ . In Table III we give the following parameters for the SIM in the calculated nuclei; the total SIM strength  $\bar{m}_{\mu}(0)$ , the average energy  $\bar{E}_{\mu} = \bar{m}_{\mu}(1)/\bar{m}_{\mu}(0)$ , the energy at maximum response, and the full width at half maximum (FWHM) of the strong peak of the SIM. We note that  $\bar{m}_{+1}(0) > \bar{m}_{-1}(0)$ , although  $N > Z$ . This inequality is due to the fact that a very large part of the excess neutron-transition strength for the operator  $\bar{Q}_{0,1^+, -1}$  goes to the  $GT$ ; hence, the

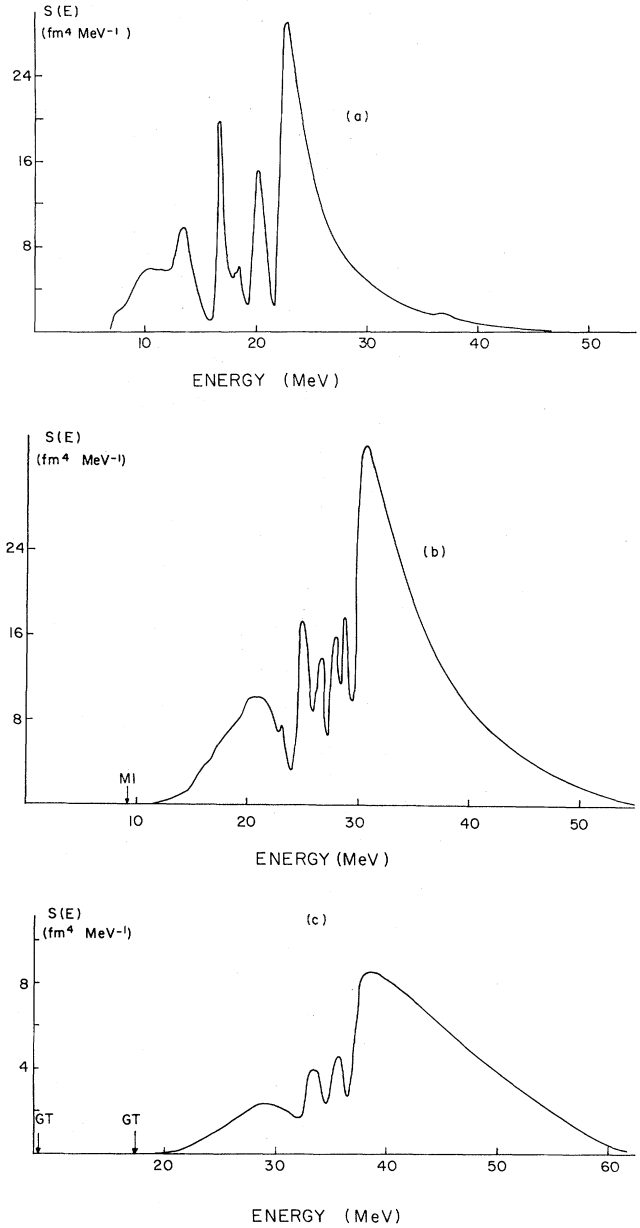


FIG. 3. Distribution of the SIM strength in  $^{90}\text{Zr}$ : (a) the  $\mu=+1$  strength, (b) the  $\mu=0$  strength, and (c) the  $\mu=-1$  strength. The locations of the  $GT$  and  $M1$  states are also indicated.

$\mu=-1$  and  $+1$  SIM resonances are built mainly from excitations of the *core* neutrons and protons, respectively. Referring to the NEWSR of Eq. (2.11), and using

TABLE III. The SIM resonances: strength, average excitation energies, energies of the main peak, and FWHM.

Nucleus	$\mu=+1$				$\mu=0$				$\mu=-1$			
	$\bar{m}(0)$ ( $\text{fm}^6$ )	$\bar{E}$ (MeV)	$E_{\text{peak}}$ (MeV)	FWHM (MeV)	$\bar{m}(0)$ ( $\text{fm}^6$ )	$\bar{E}$ (MeV)	$E_{\text{peak}}$ (MeV)	FWHM (MeV)	$\bar{m}(0)$ ( $\text{fm}^6$ )	$\bar{E}$ (MeV)	$E_{\text{peak}}$ (MeV)	FWHM (MeV)
$^{60}\text{Ni}$	182.8	26.7	24.5	4.0	174.8	34.4	32.0	8.5	144.9	45.7	39.7	13.0
$^{90}\text{Zr}$	460.9	22.3	22.8	3.0	404.3	32.3	30.5	6.0	298.3	43.4	38.5	12.0
$^{208}\text{Pb}$	1546.6	17.7	17.8	1.0	1920.5	27.7	28.7	4.5	1184.0	44.5	42.5	12.5

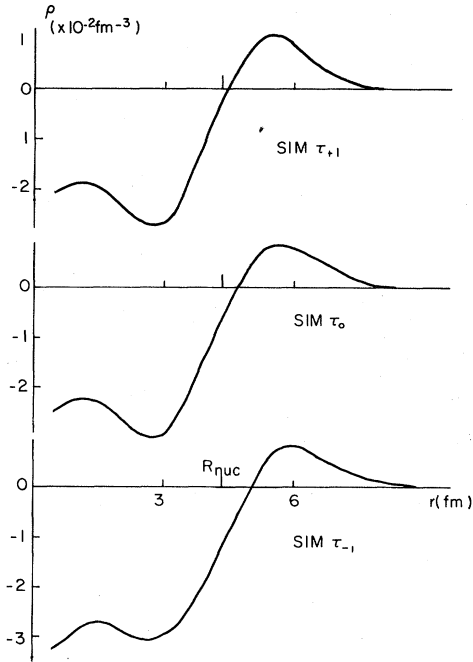


FIG. 4. The transition densities for the main peaks of the SIM distributions in  $^{90}\text{Zr}$ .

$f(r)=r^2$ , we see that the difference  $\bar{m}_{-1}(0)-\bar{m}_{+1}(0)$  should be approximately proportional to the differences between the core neutrons and core protons  $\langle r^4 \rangle$  moments. This difference is negative due to the Coulomb polarization phenomenon<sup>40</sup> of the core protons.

As a typical example, we show in Fig. 4 the transition densities for the main peaks of the SIM in  $^{90}\text{Zr}$ . The densities are normalized to the total SIM strength,  $\bar{m}_\mu(0)$ . Again, the resemblance to the electric monopole transition density<sup>14</sup> is striking.

To end the discussion of the SIM, we should mention that this resonance may play a role in the scattering amplitude of nucleon-nucleus reactions even at forward angles. As an example, we quote here the results of a calculation carried out for the following operator:

$$Q'_{0,1+,0} = \sum_{i=1}^A j_0(qr_i) [Y_{00}(r_i) \times \vec{\sigma}(i)]_{1,0} \tau_0(i), \quad (3.4)$$

where  $q$  is the proton momentum transfer in the reaction  $^{90}\text{Zr}(p,p')$  for  $\theta=3.5^\circ$  and for an incoming proton energy of 318 MeV. This reaction was recently studied experimentally.<sup>41</sup> (Note that  $q$  depends on the nuclear excitation energy.) The results, in the framework of the plane-wave approximation, are that the SIM carries about 30% of the total strength, and the rest is contained in the  $M1$  state, which is theoretically<sup>11</sup> predicted to be located at 9.15 MeV.

In view of this result we should point out that if additional  $L=0$  strength is found at higher energies in the continuum<sup>39</sup> it does not necessarily mean that GT strength of the kind given by the operator  $Q_{0,1+,-1}$  is recovered. It could be that the observed  $L=0$  transitions correspond to the SIM strength given by the operator  $\bar{Q}_{0,1+,-1}$ .

### C. Results for $L=1$ states

The probing operators are defined as follows:

$$Q_{1,J,\mu} = -(-1)^J \sum_{i=1}^A r_i [Y_1(\hat{r}_i) \times \vec{\sigma}(i)]_{J,0} r_\mu(i) \quad (3.5)$$

and the possible excitations may possess the spins  $J^\pi=0^-,1^-,2^-$ . The resulting total strengths,  $m_{1,J,\mu}(0)$ , and average excitation energies,

$$E_{1,J,\mu} = m_{1,J,\mu}(1)/m_{1,J,\mu}(0),$$

for all values of  $J$  are listed in Table IV. In Table V are given the average excitation energies for the three isospin modes with  $L=1$ . These energies have been defined as

$$E_{L,\mu} = \frac{\sum_{J=0}^2 (2J+1) m_{1,J,\mu}(1)}{\sum_{J=0}^2 (2J+1) m_{1,J,\mu}(0)}. \quad (3.6)$$

The results of Table IV were checked against the NEWSR derived in Sec. IIB. In Table VI, we give the values of the sum rules, calculated using HF densities. These sum

TABLE IV. The  $L=1, S=1$  states: total strengths and average excitation energies for the different values of the angular momentum  $J$ .

Nucleus	$J^\pi$	$\mu=+1$		$\mu=0$		$\mu=-1$	
		$m_{1,J,+1}(0)$ (fm <sup>2</sup> )	$E_{1,J,+1}$ (MeV)	$m_{1,J,0}(0)$ (fm <sup>2</sup> )	$E_{1,J,0}$ (MeV)	$m_{1,J,-1}(0)$ (fm <sup>2</sup> )	$E_{1,J,-1}$ (MeV)
$^{60}\text{Ni}$	$0^-$	26.9	18.9	31.6	26.0	36.6	32.7
	$1^-$	21.6	15.5	25.9	22.1	31.4	29.0
	$2^-$	10.6	12.1	18.0	17.4	21.4	24.5
$^{90}\text{Zr}$	$0^-$	28.2	12.5	41.5	22.7	60.4	31.8
	$1^-$	23.7	10.3	33.5	19.9	55.1	28.4
	$2^-$	12.7	9.1	24.9	16.6	42.9	23.5
$^{208}\text{Pb}$	$0^-$	19.2	12.5	130.3	20.3	266.1	32.1
	$1^-$	20.2	7.6	108.3	16.9	233.3	29.5
	$2^-$	11.8	14.4	50.4	14.3	216.2	25.1

TABLE V. The  $L=1, S=1$  average energies.

Nucleus	$\mu=+1$	$\mu=0$	$\mu=-1$
	$E_{1,+1}$ (MeV)	$E_{1,0}$ (MeV)	$E_{1,-1}$ (MeV)
$^{60}\text{Ni}$	14.9	20.6	27.5
$^{90}\text{Zr}$	10.2	18.8	26.5 <sup>a</sup> 24.9 <sup>b</sup>
$^{208}\text{Pb}$	11.2	16.6	27.5 <sup>a</sup> 24.5 <sup>b</sup>

<sup>a</sup>Theoretical.<sup>b</sup>Experimental (Ref. 4).

rules are satisfied quite well by the RPA calculations as indicated by the numbers of percents. We note that, for a given  $J$ , the  $\mu=+1$  transition strength is the lowest in magnitude and the  $\mu=-1$  strength is the highest. This is due to the excess neutrons which, because of the Pauli exclusion principle, block some of the  $\Delta\tau_z=+1$  type transitions, and also increase the number of configurations contributing to the  $\mu=-1$  mode over that of the  $\mu=0$  or  $+1$  modes. The influence of the excess neutrons is, of course, quite pronounced in the case of  $^{208}\text{Pb}$ . For this nucleus, the  $1^-, \Delta\tau_z=-1$  strength is about ten times larger than that of the  $1^-, \Delta\tau_z=+1$  mode. For the latter strength, we quote only the contribution of low energy states; the ones at higher energy add about 10% more strength, which is centered around 28 MeV. As for the  $2^-$  excitations in  $^{208}\text{Pb}$ , the  $\mu=-1$  total strength is about 18 times that of the  $\mu=+1$  mode. The  $2^-, \mu=+1$  strength is distributed as follows: two narrow states, one at 7.0 MeV and the other at 9.7 MeV, carry together about 70% of the strength; the remaining 30% is spread over an interval of 25 MeV, and centered around 27 MeV. (In view of this behavior, one should not attach much significance to the average energy  $E_{1,2^-,+1}$  in the case of  $^{208}\text{Pb}$ .)

We also note that for  $L=1$  transitions involving

TABLE VI. Sum rules for  $L=1, S=1$  excitations. The values of the sum rules calculated using HF densities are given for each spin. The percentage figures represent the extent to which these sum rules are exhausted by the RPA calculations.

Nucleus	$^{60}\text{Ni}$	$^{90}\text{Zr}$	$^{208}\text{Pb}$
$J^\pi$		$0^-$	
Charge exchange NEWSR	10.0 97%	32.4 99%	241.1 102%
$J^\pi$		$1^-$	
Charge exchange NEWSR	10.0 98%	32.4 97%	241.1 88%
$J^\pi$		$2^-$	
Charge exchange NEWSR	10.0 108%	32.4 93%	241.1 85%

$\Delta\tau_z=-1$  and  $0$ , the average energy of  $0^-$  excitations is the highest, and that of  $2^-$  excitations is the lowest. This feature has been noted also in previous calculations.<sup>18,42</sup> The authors of Ref. 18 attribute the fact that the theoretical energy of the  $0^-$  excitation is the highest mainly to the one-body spin-orbit potential; the configurations which contribute most of the  $0^-$  strength have larger unperturbed energies than those of importance for the  $1^-, 2^-$  resonances. The above mentioned energy ordering does not hold for the  $\Delta\tau_z=+1$  states in  $^{108}\text{Pb}$  because of the Pauli blocking resulting from the excess neutrons. The strength for  $J^\pi=0^-, 1^-$  in all three nuclei is concentrated in very few peaks,<sup>18</sup> while the  $J^\pi=2^-$  strength is spread

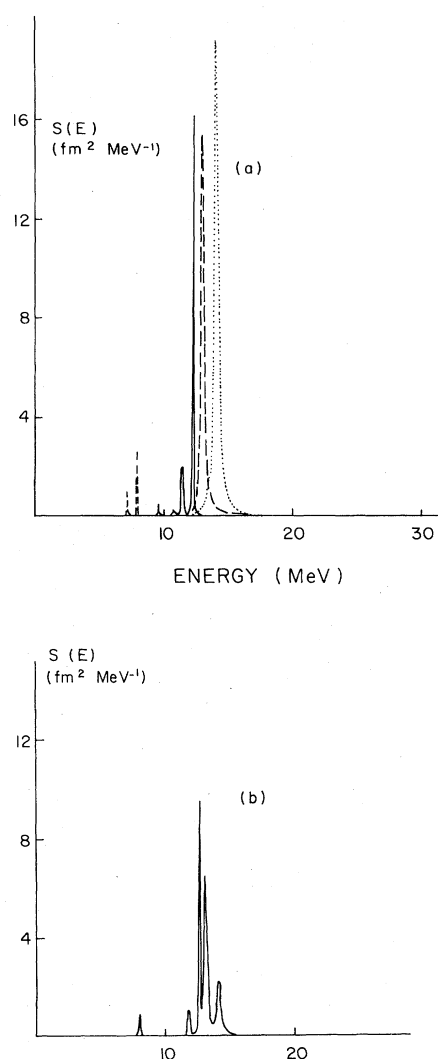


FIG. 5. The  $L=1, \mu=+1$  distribution of strength in  $^{90}\text{Zr}$ . (a) The strength distributions for the  $J=0^-$  (dotted line),  $J=1^-$  (dashed line), and  $J=2^-$  (continuous line) are shown. (b) The distribution of the "average strength"

$$S_{L,\mu} = \frac{\sum_J (2J+1) S_{L,J,\mu}}{3(2L+1)}$$

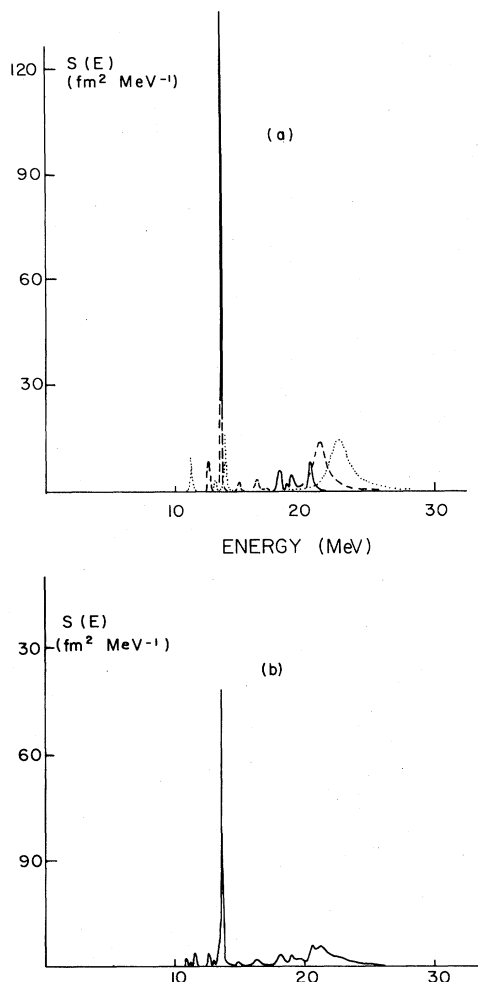


FIG. 6. The  $L=1, \mu=0$  distribution of strength in  $^{90}\text{Zr}$ . See the caption of Fig. 5.

over many states. The  $\mu=-1$  strengths for all  $L=1$  states have smoother distributions than the corresponding  $\mu=0, \mu=+1$  states, because of the higher energies and thus larger escape widths. The  $L=1$  strength, defined as

$$S_{1,\mu}(E) = \frac{\sum_{J=0}^2 (2J+1) S_{1,J,\mu}(E)}{9}, \quad (3.7)$$

where  $S_{1,J,\mu}(E)$  is the transition strength for the operator  $Q_{1,J,\mu}$  at energy  $E$ , is quite fragmented and spread over an energy interval of 5–7 MeV for the  $\mu=+1$  mode (disregarding the high energy strength  $\mu=+1, J^\pi=1^-, 2^-$  in  $^{208}\text{Pb}$ ), and over an interval 15–25 MeV for the  $\mu=0, \mu=-1$  modes. In Figs. 5–7 we show the  $J^\pi=0^-, 1^-, 2^-$  strength distributions and the total  $L=1$  distribution for all three isospin modes in  $^{90}\text{Zr}$ . The above mentioned features are well illustrated in these figures. In Figs. 8–10 are shown the transition densities for the main peaks of the  $L=1$  distributions in  $^{90}\text{Zr}$ . For reasons of comparison, the transition densities are normalized to the corresponding strengths. We note that the densities are peaked at the nuclear surface.

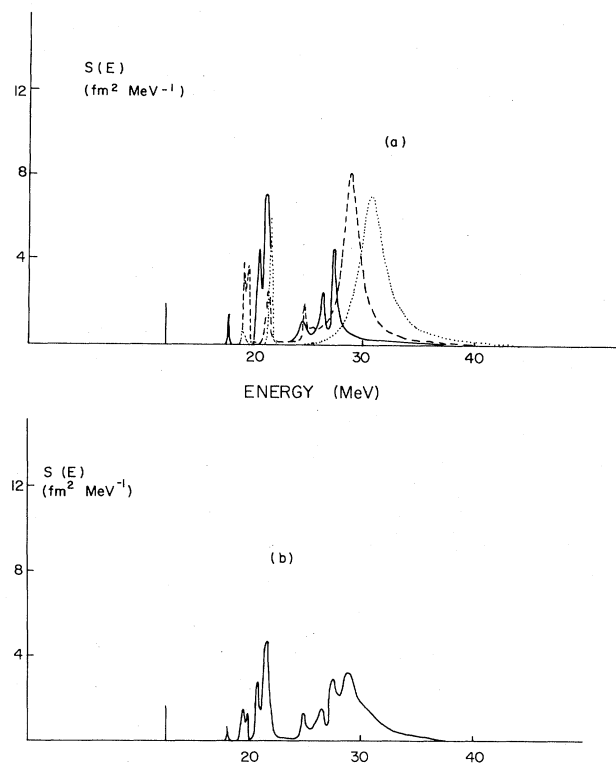


FIG. 7. The  $L=1, \mu=-1$  distribution of strength in  $^{90}\text{Zr}$ . See the caption of Fig. 5.

It is interesting to estimate the influence of the RPA correlations in the  $L=1$  excitations. As shown in Ref. 11, the RPA correlations are insignificant for the GT states in  $^{90}\text{Zr}$  and  $^{108}\text{Pb}$ , while the resulting reduction in the GT strength for  $^{60}\text{Ni}$  is 23%, compared to the TDA strength. For  $L=1$  states the RPA correlations are very important. In Table VII, we give the results of TDA calculations of  $L=1$  states in  $^{90}\text{Zr}$ . We note that the RPA strengths of the  $\mu=-1$  modes are smaller than the TDA ones by about 20% and, for the  $\mu=+1$  mode, the RPA

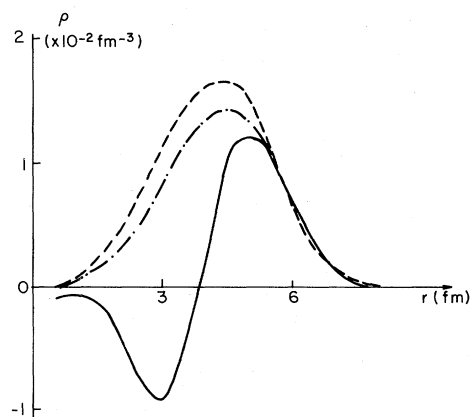
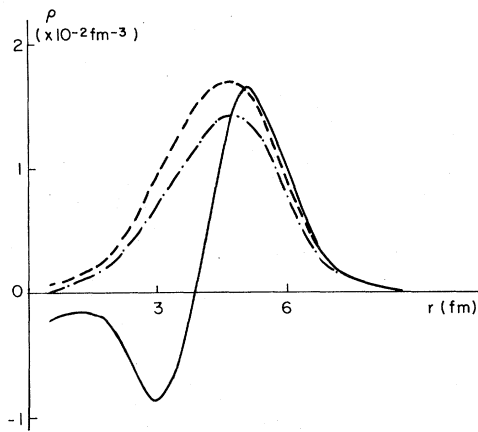


FIG. 8. Transition densities for the main peaks of the  $L=1, \mu=+1$  distribution in  $^{90}\text{Zr}$ . The dashed, dashed-dotted, and continuous lines represent the  $0^-, 1^-,$  and  $2^-$  densities, respectively.

FIG. 9. Same as Fig. 8 for  $L=1, \mu=0$ .

correlations reduce the TDA strength by about 50%. The relative reduction in strength caused by the RPA correlations is higher for  $\mu=1$  than for  $\mu=-1$  transitions.<sup>14</sup> Also, for the  $\mu=0$  modes, the RPA strengths are only about 70–80% of the TDA ones. The TDA average energies are higher than the corresponding RPA ones by 1.5–2 MeV.

#### D. Comparison with experiment

The  $L=1, S=1$  resonances were observed in (p,n) reactions with several targets,<sup>4,35</sup> including  $^{90}\text{Zr}$  and  $^{208}\text{Pb}$ . The measured<sup>4</sup>  $L=1, \mu=-1$  energy in  $^{90}\text{Zr}$  is 24.9 MeV, while our calculations yield 26.5 MeV. In  $^{208}\text{Pb}$ , the experimental value of  $E_{1,-1}$  is 24.5 MeV and the calculated one is 27.5 MeV. The agreement between measurement and theory is only slightly improved if we compare the energies of the  $T_{<}=T-1$  components,<sup>18</sup> assuming that the experiment includes only the  $T_{<}$  strength. The calculated values of the  $T_{<}$  centroid energies<sup>14</sup> are 25.8 MeV for  $^{90}\text{Zr}$  and 27.2 MeV for  $^{208}\text{Pb}$ . There is additional data concerning  $^{208}\text{Pb}$ : a low-lying  $2^-, \mu=-1$  state at 6.3 MeV has been reported in Ref. 4. We also find a bound state at 7.3 MeV which possesses about 5% of the total calculated  $2^-$  strength. In the very recent experimental study of the  $^{90}\text{Zr}(p,p')$  reaction,<sup>41</sup> a concentration of strength was observed around an excitation energy of 18 MeV. The theoretical result of  $E_{1,0}=18.8$  MeV indicates that the observed strength could be of  $L=1, S=1$  nature.

TABLE VII. The  $L=1, S=1$  strengths and average excitation energies in  $^{90}\text{Zr}$ , calculated using the TDA.

$J$	$\mu=+1$		$\mu=0$		$\mu=-1$	
	$m_{1,J,+1}(0)$ (fm <sup>2</sup> )	$E_{1,J,+1}$ (MeV)	$m_{1,J,0}(0)$ (fm <sup>2</sup> )	$E_{1,J,0}$ (MeV)	$m_{1,J,-1}(0)$ (fm <sup>2</sup> )	$E_{1,J,-1}$ (MeV)
$0^-$	43.3	14.2	57.2	24.2	73.4	33.6
$1^-$	36.2	11.9	50.0	20.8	64.9	30.3
$2^-$	23.0	9.9	31.5	17.4	52.4	24.8

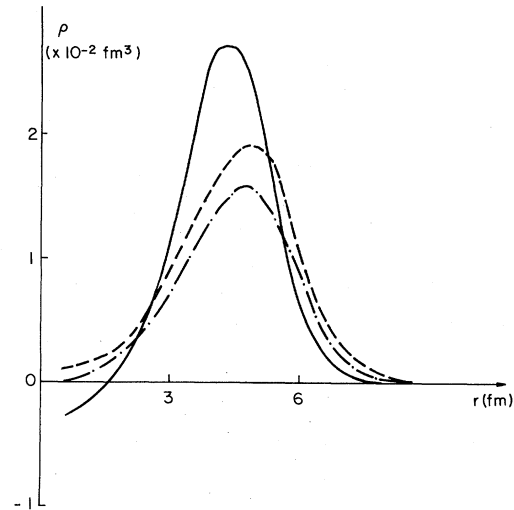
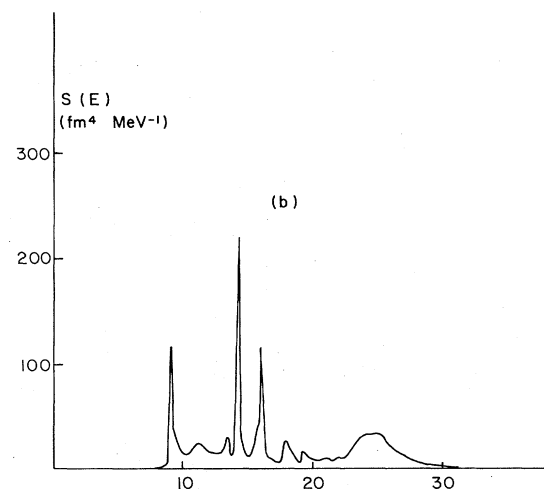
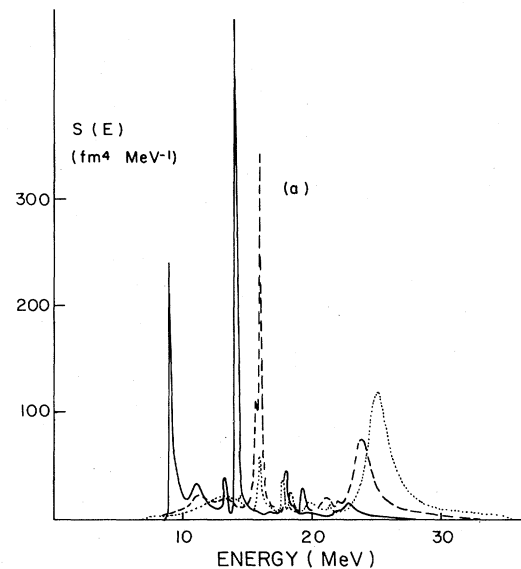
FIG. 10. Same as Fig. 8 for  $L=1, \mu=-1$ .

FIG. 11. The  $L=2, \mu=+1$  distribution of strength in  $^{90}\text{Zr}$ . (a) The strength distributions for the  $J=1^+$  (dotted line),  $J=1^-$  (dashed line), and  $J=3^+$  (continuous line) are shown. (b) The distribution of the "average strength" (see Fig. 5).

TABLE VIII. The  $L=2, S=1$  states (see the caption of Table IV).

Nucleus	$J$	$\mu=+1$		$\mu=0$		$\mu=-1$	
		$m_{2,J,+1}(0)$ (fm <sup>4</sup> )	$E_{2,J,+1}$ (MeV)	$m_{2,J,0}(0)$ (fm <sup>4</sup> )	$E_{2,J,0}$ (MeV)	$m_{2,J,-1}(0)$ (fm <sup>4</sup> )	$E_{2,J,-1}$ (MeV)
<sup>60</sup> Ni	1 <sup>+</sup>	670.9	29.5	760.0	35.5	914.3	39.0
	2 <sup>+</sup>	587.8	23.4	743.6	26.6	849.0	33.5
	3 <sup>+</sup>	429.6	17.0	508.4	23.2	656.7	27.1
<sup>90</sup> Zr	1 <sup>+</sup>	1047.3	22.9	1445.1	32.5	1852.3	40.1
	2 <sup>+</sup>	950.7	19.8	1283.8	27.7	1736.6	35.1
	3 <sup>+</sup>	800.0	14.6	967.8	22.8	1563.5	28.5
<sup>208</sup> Pb	1 <sup>+</sup>	3343.8	20.2	7567.9	27.9	12733.6	36.8
	2 <sup>+</sup>	2507.4	13.8	6113.1	23.9	11189.4	34.7
	3 <sup>+</sup>	1419.1	13.3	4366.0	19.3	10236.5	28.9

E. Results for  $L=2$  states

The operators inducing this kind of excitations are taken to be

$$Q_{2,J,\mu} = (-i)^{J+1} \sum_{i=1}^A r_i^2 [Y_2(\hat{r}_i) \times \vec{\sigma}(i)]_{J,0} \tau_\mu(i), \quad (3.8)$$

and we have to deal with states of  $J^\pi = 1^+, 2^+, \text{ and } 3^+$ .

In Table VIII are shown the total strengths  $m_{2,J,\mu}(0)$  and the average energies  $E_{2,J,\mu}$  for all possible values of  $J$ , and in Table IX are listed the average energies of the  $L=2$  resonances [see Eq. (3.6)]. The NEWSR of Sec. II are satisfied within 85–100%. As in the previous case of  $L=1$  states, the magnitudes of the transition strengths for a given  $J$  are affected by the excess neutrons. However, here the Pauli blocking effect is considerably weaker, because the  $L=2$  states are composed of p-h transitions essentially of  $2\hbar\omega$  excitation energy, and not  $1\hbar\omega$  as those participating in the  $L=1$  resonances. The largest ratio between the  $\Delta\tau_z = -1$  strength and the  $\Delta\tau_z = +1$  one occurs for the  $3^+$  excitations in <sup>208</sup>Pb, and its value is about 7, compared to

$$m_{1,2^-, -1}(0)/m_{1,2^-, +1}(0) \approx 18$$

for the same nucleus.

We also note that the energy ordering of the  $L=2$

TABLE IX. The  $L=2, S=1$  average energies.

Nucleus	$\mu=+1$	$\mu=0$	$\mu=-1$
	$E_{2,+1}$ (MeV)	$E_{2,0}$ (MeV)	$E_{2,-1}$ (MeV)
<sup>60</sup> Ni	22.5	27.4	32.3
<sup>90</sup> Zr	18.4	27.0	33.3 <sup>a</sup> 31.0 <sup>b</sup>
<sup>208</sup> Pb	15.6	23.3	32.7 <sup>a</sup> 31.5 <sup>b</sup>

<sup>a</sup>Theoretical.

<sup>b</sup>Experimental (Ref. 4).

states involving  $\Delta\tau_z = +1, 0, -1$  transitions is such that the  $1^+$  excitation is the highest in energy and the  $3^+$  excitation is the lowest. The explanation is similar to that quoted<sup>18</sup> for the energy ordering of the  $L=1$  states. This feature is weakened by the Pauli blocking in the case of the  $L=2, \mu=+1$  excitations.

The distributions of strength for the  $L=2, J=1^+$  resonances are such that a few peaks carry most of the strength, while the  $J=2^+, 3^+$  distributions are very much fragmented. The  $L=2$  strength, defined in analogy with Eq. (3.7), extends over a broad energy domain: For the  $\mu=+1$  mode, the strength is spread over about 25 MeV and for the other two modes it covers an interval ranging

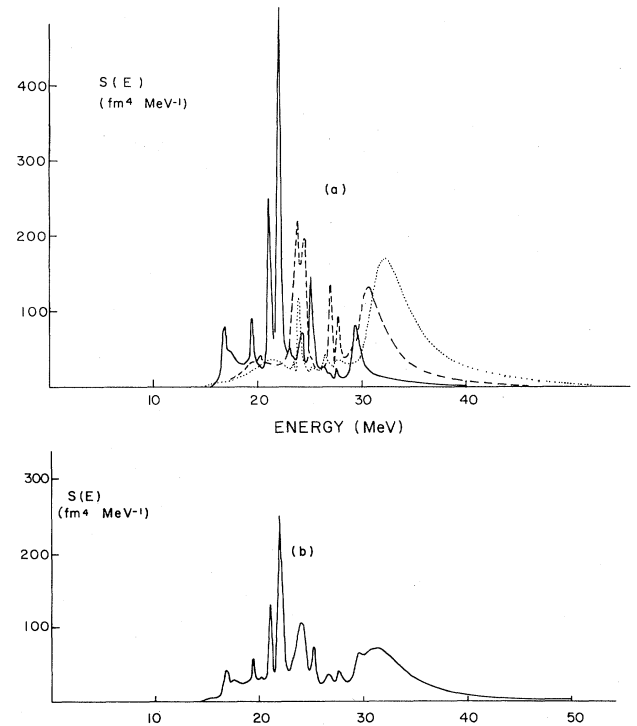


FIG. 12. The  $L=2, \mu=0$  distribution of strength in <sup>90</sup>Zr. See the caption of Fig. 11.

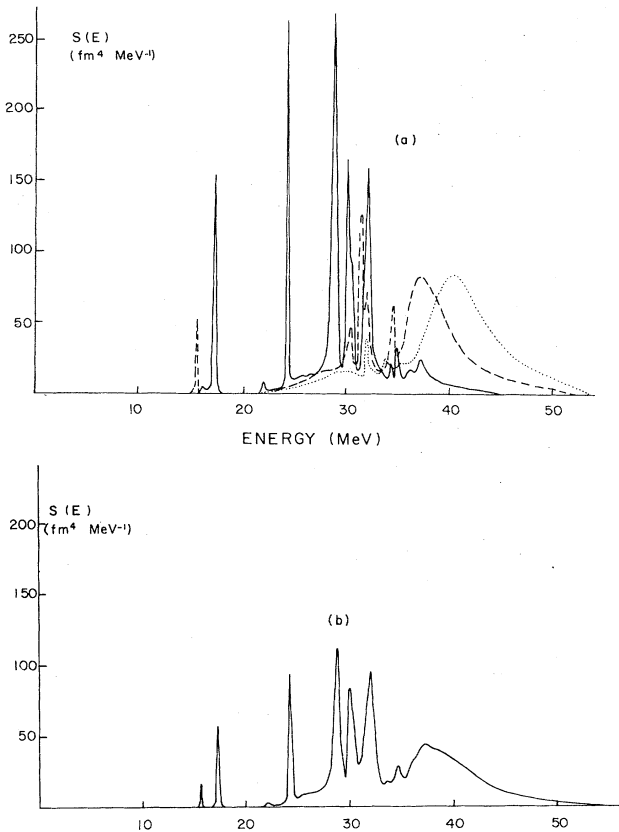


FIG. 13. The  $L=2, \mu=-1$  distribution of strength in  $^{90}\text{Zr}$ . See the caption of Fig. 11.

between 35–45 MeV. The  $L=2$  distributions of all three isospin modes exhibit a wide peak at their high energy end; this peak exhausts a significant fraction of the corresponding strength. As illustrative examples, in Figs. 11–13 are shown the  $L=2$  distributions calculated for  $^{90}\text{Zr}$ .

#### F. Comparison with experiment

The observation of the  $L=2, S=1, \Delta\tau_z=-1$  resonances in the (p,n) reaction at  $E_p=200$  MeV has been reported.<sup>4</sup> In  $^{90}\text{Zr}$ , the  $L=2$  strength was experimentally estimated to lie at 31 MeV, while theory yields

$E_{2,-1}=33.3$  MeV. In  $^{208}\text{Pb}$  the agreement is even better: the measured<sup>4</sup> value of  $E_{2,-1}$  is 31.5 MeV and the theoretical one is 32.7 MeV.

The experimental findings<sup>41</sup> in the  $^{90}\text{Zr}(p,p')^{90}\text{Zr}^*$  reaction that a substantial amount of spin-flip strength exists between 7 and 25 MeV excitation energy is completely consistent with the present theoretical results. The calculated combined  $L=0,1,2$  spin-flip strength is spread over that region of excitation and even beyond the 25 MeV excitation energy.

#### IV. SUMMARY

In this work, we calculated the strength distributions of all three isospin components of magnetic isovector states in several  $N > Z$  nuclei. We employed the continuum HF-RPA framework. The residual interaction was taken to be of zero range.

The resulting strength distributions for excited states of orbital angular momentum values  $L=0,1,2$  were computed. The high energy  $L=0$  type of concentration of strength (the spin isovector monopole) was also studied. The role played by the excess neutrons in  $N > Z$  nuclei was investigated in detail.

A considerable energy splitting for the various  $J$  values was found for  $L > 0$  states. For a given  $L$ , this splitting, which is due to the spin orbit interaction, results in the lowest  $J$  state having the highest energy.

The calculated excitation energies are in reasonable agreement with the experimental energies for levels that were observed. More experimental data, particularly of the kind in which  $L > 0$  states of  $\Delta\tau_z=0$  and  $+1$  type, are needed so as to make comparison with theory more complete. It is of special interest to detect the spin-isovector-monopole resonance. The (p,n) and ( $^3\text{He},t$ ) reaction could be used but the charge-conjugate reactions (n,p) and ( $t,^3\text{He}$ ) seem to be even more promising.

#### ACKNOWLEDGMENTS

We wish to thank N. Anantaraman, J. D. Bowman, G. M. Crawley, W. G. Love, J. Rapaport, and L. Zamick for helpful discussions. One of us (N.A.) wishes to thank Louis Rosen for the kind hospitality at Los Alamos. This work was supported in part by the U.S. Department of Energy.

<sup>1</sup>C. D. Goodman, Nucl. Phys. **A374**, 241 (1982), and references therein.  
<sup>2</sup>N. Anantaraman *et al.*, Phys. Rev. Lett. **46**, 1318 (1981); Y. Fujita *et al.*, Phys. Rev. C **25**, 678 (1982).  
<sup>3</sup>G. Eulenberg *et al.*, Phys. Lett. **116B**, 113 (1982); A. Richter, Nucl. Phys. **A374**, 177c (1982).  
<sup>4</sup>C. Gaarde *et al.*, Nucl. Phys. **A369**, 258 (1981).  
<sup>5</sup>W. G. Love and M. A. Franey, Phys. Rev. C **24**, 1073 (1981).  
<sup>6</sup>G. M. Crawley *et al.*, Phys. Rev. C **26**, 87 (1982).  
<sup>7</sup>C. Djalali *et al.*, Nucl. Phys. **A338**, 1 (1982).  
<sup>8</sup>M. Ericson, A. Figureau, and C. Thévenet, Phys. Lett. **45B**, 19 (1973); E. Oset and M. Rho, Phys. Rev. Lett. **42**, 47 (1979); I. S. Towner and F. C. Khanna, *ibid.* **42**, 51 (1979); G. F. Bertsch, Nucl. Phys. **A354**, 157 (1981); H. Toki and W.

Weise, Phys. Lett. **97B**, 12 (1980); A. Bohr and B. R. Mottelson, *ibid.* **100B**, 10 (1981); G. E. Brown and M. Rho, Nucl. Phys. **A372**, 397 (1981).  
<sup>9</sup>K. Shimizu, M. Ichimura, and A. Arima, Nucl. Phys. **A226**, 282 (1974).  
<sup>10</sup>F. Osterfeld, Phys. Rev. C **26**, 762 (1982).  
<sup>11</sup>N. Auerbach, L. Zamick, and A. Klein, Phys. Lett. **118B**, 256 (1982).  
<sup>12</sup>G. F. Bertsch and I. Hamamoto, Phys. Rev. **C26**, 1323 (1982).  
<sup>13</sup>W. Knapfner and B. C. Metsch, in *Proceedings of the International Symposium on Highly Excited States and Nuclear Structure*, edited by N. Marty and Nguyen Van Giai (Les Editions de Physique, Paris, 1983).  
<sup>14</sup>N. Auerbach and Amir Klein, Nucl. Phys. **A395**, 77 (1983).

- <sup>15</sup>S. Shlomo and G. F. Bertsch, Nucl. Phys. **A243**, 507 (1975);  
K. F. Liu and Nguyen Van Giai, Phys. Lett. **65B**, 23 (1976).
- <sup>16</sup>D. Vautherin and D. M. Brink, Phys. Rev. C **5**, 626 (1972).
- <sup>17</sup>M. Beiner *et al.*, Nucl. Phys. **A238**, 29 (1975).
- <sup>18</sup>G. F. Bertsch, D. Cha, and H. Toki, Phys. Rev. C **24**, 533 (1981).
- <sup>19</sup>J. Speth *et al.*, Nucl. Phys. **A343**, 382 (1980).
- <sup>20</sup>B. A. Brown and B. H. Wildenthal, Phys. Rev. C **27**, 1296 (1983).
- <sup>21</sup>T. Izumoto, Nucl. Phys. **A395**, 189 (1983).
- <sup>22</sup>D. J. Thouless, *The Quantum Mechanics of Many-Body Problems* (Academic, New York, 1961); Nucl. Phys. **22**, 78 (1961).
- <sup>23</sup>N. Auerbach and Amir Klein, Phys. Rev. C **28**, 2075 (1983).
- <sup>24</sup>A. Bohr and B. R. Mottelson, *Nuclear Structure* (Benjamin, New York, 1969), Vol. I.
- <sup>25</sup>G. F. Bertsch and S. F. Tsai, Phys. Rep. **18C**, 125 (1973).
- <sup>26</sup>K. F. Liu and G. E. Brown, Nucl. Phys. **A265**, 385 (1976).
- <sup>27</sup>S. O. Bäckman, A. D. Jackson, and J. Speth, Phys. Lett. **56B**, 209 (1975).
- <sup>28</sup>G. E. Brown *et al.*, Nucl. Phys. **A286**, 191 (1977); S. O. Bäckman *et al.*, *ibid.* **A345**, 202 (1980).
- <sup>29</sup>Nguyen Van Giai and H. Sagawa, Phys. Lett. **106B**, 379 (1981).
- <sup>30</sup>D. E. Bainum *et al.*, Phys. Rev. Lett. **44**, 1751 (1980).
- <sup>31</sup>H. Toki, G. F. Bertsch, and D. Cha, Phys. Rev. C **28**, 1398 (1983).
- <sup>32</sup>K. Weinhard *et al.*, Phys. Rev. Lett. **49**, 18 (1982); S. I. Hayakawa *et al.*, *ibid.* **49**, 1624 (1982).
- <sup>33</sup>J. Meyer-ter-Vehn, Phys. Rep. **74C**, 323 (1981), and references therein.
- <sup>34</sup>J. Speth *et al.*, Nucl. Phys. **343**, 382 (1980).
- <sup>35</sup>D. J. Horen *et al.*, Phys. Lett. **99B**, 383 (1981).
- <sup>36</sup>J. Rapaport *et al.*, Phys. Lett. **119B**, 61 (1982).
- <sup>37</sup>N. Anantaraman *et al.* (unpublished).
- <sup>38</sup>J. Speth *et al.*, Phys. Lett. **63B**, 257 (1975).
- <sup>39</sup>O. Scholten, G. F. Bertsch, and H. Toki, Phys. Rev. C **27**, 2975 (1983); G. F. Bertsch and O. Scholten, *ibid.* **25**, 804 (1983).
- <sup>40</sup>E. H. Auerbach, S. Kahana, and J. Weneser, Phys. Rev. Lett. **23**, 1253 (1969); N. Auerbach, Phys. Lett. **36B**, 293 (1971); L. Zamick, *ibid.* **39B**, 241 (1972).
- <sup>41</sup>S. K. Nanda *et al.*, Phys. Rev. Lett. **51**, 1526 (1983).
- <sup>42</sup>F. Krmpotic, K. Ebert, and W. Wild, Nucl. Phys. **A342**, 497 (1980).